Acta Pharmacologica Sinica

www.nature.com/aps

ARTICLE

Activated SIRT1 contributes to DPT-induced glioma cell parthanatos by upregulation of NOX2 and NAT10

Shi-peng Liang[1,2], Xuan-zhong Wang[1,2], Mei-hua Piao[3], Xi Chen[1,2], Zhen-chuan Wang[1,2], Chen Li[1,2], Yu-bo Wang[1], Shan Lu[1], Chuan He[1], Yan-li Wang[2,4], Guang-fan Chi[5] and Peng-fei Ge[1,2]✉

Parthanatos is a type of programmed cell death dependent on hyper-activation of poly (ADP-ribose) polymerase 1 (PARP-1). SIRT1 is a highly conserved nuclear deacetylase and often acts as an inhibitor of parthanatos by deacetylation of PARP1. Our previous study showed that deoxypodophyllotoxin (DPT), a natural compound isolated from the traditional herb *Anthriscus sylvestris*, triggered glioma cell death via parthanatos. In this study, we investigated the role of SIRT1 in DPT-induced human glioma cell parthanatos. We showed that DPT (450 nmol/L) activated both PARP1 and SIRT1, and induced parthanatos in U87 and U251 glioma cells. Activation of SIRT1 with SRT2183 (10 μmol/L) enhanced, while inhibition of SIRT1 with EX527 (200 μmol/L) or knockdown of SIRT1 attenuated DPT-induced PARP1 activation and glioma cell death. We demonstrated that DPT (450 nmol/L) significantly decreased intracellular NAD^+ levels in U87 and U251 cells. Further decrease of NAD^+ levels with FK866 (100 μmol/L) aggravated, but supplement of NAD^+ (0.5, 2 mmol/L) attenuated DPT-induced PARP1 activation. We found that NAD^+ depletion enhanced PARP1 activation via two ways: one was aggravating ROS-dependent DNA DSBs by upregulation of NADPH oxidase 2 (NOX2); the other was reinforcing PARP1 acetylation via increase of N-acetyltransferase 10 (NAT10) expression. We found that SIRT1 activity was improved when being phosphorylated by JNK at Ser27, the activated SIRT1 in reverse aggravated JNK activation via upregulating ROS-related ASK1 signaling, thus forming a positive feedback between JNK and SIRT1. Taken together, SIRT1 activated by JNK contributed to DPT-induced human glioma cell parthanatos via initiation of NAD^+ depletion-dependent upregulation of NOX2 and NAT10.

Keywords: glioma; parthanatos; PARP1; SIRT1; NAT10; NOX2

Acta Pharmacologica Sinica (2023) 44:2125–2138; https://doi.org/10.1038/s41401-023-01109-3

INTRODUCTION

Parthanatos is a type of programmed cell death dependent on hyper-activation of poly (ADP-ribose) polymerase 1 (PARP-1) [1]. Hyper-activated PARP1 primarily leads to cell death via two pathways. The first one is consuming nicotinamide adenine dinucleotide (NAD^+) to produce poly(ADP-ribose) (PAR) polymers, which target mitochondria to induce apoptosis-inducing factor (AIF) translocation from mitochondria to nuclei. Within nuclei, AIF acts as a nuclease to degrade DNA into small fragments [1]. Moreover, NAD^+ depletion resulting from the synthesis of PAR polymers could also lead to cell death by disturbing multiple biological processes such as energy metabolism, calcium homeostasis, and gene expression [2, 3]. The second one is regulating its downstream signals by adding linear or branched chains of ADP-ribose units to target proteins, a type of post-translational modification designated as PARylation [4]. Besides being involved in the pathogenesis of neurodegenerative disorders, ischemic stroke, retinal diseases, and diabetes, parthanatos is also responsible for the death induced by small molecular chemicals in various types of malignant tumors such as glioma, neuroblastoma, and oral squamous cell carcinoma [5–7]. Thus, parthanatos is emerging as a new target to eliminate malignant tumor cells.

Silent mating type information regulation 1 (SIRT1) is a highly conserved deacetylase within the nucleus and could deacetylate non-histone targets such as PARP1 and p53 [8]. Activated SIRT1 not only promotes cancer cells' growth and resistance to therapy [9, 10], but also induces cancer cell death. It was reported the autophagic death of glioma cells induced by F0911-7667, a small molecule chemical compound, was dependent on SIRT1 activation [11]. Moreover, activated SIRT1 was also found to exacerbate capsaicin-triggered lung cancer cell apoptosis and metformin-induced breast cancer cell pyroptosis [12, 13]. Therefore, SIRT1 has multiple roles in modulating cell death.

SIRT1 could be activated by NAD^+, but NAD^+ is dispensable for SIRT1 activation because post-translational modification could also have impact on SIRT1 activation [14]. SIRT1's activity is increased after being phosphorylated by JNK at Ser27. Additionally, SIRT1's stability and substrate-binding affinity were both improved after being phosphorylated [15–17]. During the course of removing acetylated lysine residues from the target proteins, activated SIRT1 cleaves NAD^+ into nicotinamide [18]. This not only decreases

[1]Department of Neurosurgery, First Hospital of Jilin University, Changchun 130021, China; [2]Research Center of Neuroscience, First Hospital of Jilin University, Changchun 130021, China; [3]Department of Anesthesiology, First Hospital of Jilin University, Changchun 130021, China; [4]Department of Obstetrics and Gynecology, First Hospital of Jilin University, Changchun 130021, China and [5]Key Laboratory of Pathobiology, Ministry of Education, Jilin University, Changchun 130021, China
Correspondence: Peng-fei Ge (gepf@jlu.edu.cn)

Received: 18 March 2023 Accepted: 9 May 2023
Published online: 5 June 2023

NAD^+ level but also boosts NAD^+ depletion-dependent ROS accumulation and DNA double strands breaks (DSBs) [19]. DNA DSBs are a canonical pathway leading to PARP1 activation, whereas SIRT1-regulated deacetylation inhibits PARP1 activation [8]. Thus, SIRT1 might exert opposite effects on parthanatos. On one hand, it inhibits PARP1 activation by the removal of the acetyl groups within PARP1. On the other hand, it reinforces PARP1 activation by triggering DNA DSBs via depletion of NAD^+. Therefore, it is needed to clarify the role of SIRT1 in parthanatos and its potential mechanisms.

Glioma is a primary malignant brain tumor with lower survival rate due to lack of effective treatments [5]. However, induction of parthanatos might become a new way of killing glioma cells because PARP1 is not only over-expressed in glioma cells [20], but also could be hyper-activated by various compounds [5–7]. We have reported that deoxypodophyllotoxin (DPT), a natural compound isolated from traditional plant *Anthriscus sylvestris*, triggered glioma cell death via parthanatos [5]. Although SIRT1 could promote cancer cells to die via different programmed death modes [11–13], its role in cancer cell parthanatos remains elusive. In this study, we used DPT to induce glioma cell parthanatos and investigated the effect of activated SIRT1 on parthanatos and its underlying mechanism.

MATERIALS AND METHODS

Reagents

DPT was obtained from Yuanye Bio-technology company (Shanghai, China). It was dissolved in DMSO and then stored at a concentration of 10 mmol/L. SRT2183 and SP600125 were both from Selleck Chemicals (Houston, TX). EX527, GSK2795039, NAD^+, FK866, and remodelin hydrobromide were all from MedChemExpress company (Shanghai, China). The primary antibodies against SIRT1(ab32441), NOX2(ab129068), acetyl-p53(ab75754), p53(ab26), phospho-ATM(Ser1981)(ab81292), phospho-H2AX(Ser139)(ab26350) and JNK (ab179461) were all from Abcam (Cambridge, UK). The antibodies against PAR (#83732), p300 (#86377), AKT (#2920), phospho-AKT(Ser473) (#4060), phospho-JNK (#4668) and β-Actin (#4970) were all from Cell Signaling Technology (Beverly, MA). The antibodies against CREB1 (bs-0035M), phospho-SIRT1(Ser27) (bs-3416R) and phospho-CREB1(Ser133) (bs-0036R) were all from Bioss antibodies company (Beijing, China). The antibodies against PARP1 (13371-1-AP), NAT10 (13365-1-AP) and pan-Acetylation(66289-1-Ig) were all from proteintech company (Wuhan, China). The other reagents were from Sigma-Aldrich.

Cell lines and culture

The human glioma U87, U251, and U118 cells obtained from Shanghai Institute of Cell Biology, Chinese Academy of Sciences were cultured at 37 °C in Dulbecco's modified Eagle's medium with high glucose, 10% fetal bovine serum, penicillin (100 U/mL) and streptomycin (100 μg/mL) in a humid environment containing 5% CO_2.

Assess of cell death by LDH release assay

A lactate dehydrogenase (LDH) release assay kit obtained from Beyotime Biotechnology (Nanjing, China) was used as reported previously by us to assay cell death [21]. The following formula was used to calculate the cell death ratio: cell death ratio (%) = $(A_{sample} - A_{control})/(A_{max} - A_{control}) \times 100$, in which A represented the absorbance value acquired by a microplate reader. A_{max} represented the absorbance value of the positive group.

Evaluation of DNA DSBs by neutral comet assay

Neutral comet assay was used as reported previously by us to detect DNA double strand breaks [22]. Briefly, the cells treated with DPT following incubation with or without EX527 and SRT2183 were examined by using neuronal comet assay. Eventually, the cells were observed with a fluorescence microscope (Olympus IX71, Tokyo, Japan). The cells with DNA comet tail were calculated and the DNA percent content in comet tail region was evaluated with Image J and OpenComet 1.3 software (four assays, each including 100 cells).

Transfection of small interfering RNA

SiRNAs were introduced to cells by Lipofectamine 3000 (Invitrogen). We obtained siRNAs targeting SIRT1 (5′-GGATGAAAGTGAAATTGAA-3′) and NAT10 (5′- GTACTCCAATATCTTTGTT-3′) from Guangzhou RiboBio (China), and targeting JNK (5′-GCCCAGUAAUAUAGUAGUATT-3′) and NOX2 (5′-CCAUGGAGCUGAACGAAUUTT-3′) and scrambled siRNA (5′-UUCUCCGAACGUGUCACGUTT-3′) from Suzhou GenePharma (China).

Immunocytochemical staining

The U87 cells treated with DPT following incubation with or without EX527 and SRT2183 were incubated with 1% Triton X-100 for 10 min following being fixed in ethanol and washed with PBS. After nonspecific binding sites were blocked, the cells were incubated overnight with the antibodies against phospho-H2AX at serine 139 (1:100) or NAT10 (1:100), then with Cy3-conjugated goat anti-rabbit IgG (1:200) for 1 h and counterstained with Hoechst33342 for 5 min. Finally, the cells were visualized by confocal microscope (Olympus FV1000, Tokyo, Japan).

Human U87 tumor xenograft in mice

The athymic BALB/c nude mice (4 weeks; 20–22 g) purchased from Beijing Vital River laboratory were housed under a twelve hours light and dark cycle with free access to water and food. The environment was pathogen-free and the research protocol was approved by the ethics committee of the first hospital of Jilin University (Changchun, China). After three days acclimatization to the environment, the mice were subcutaneously injected with U87 cells (1×10^6) in 100 μL PBS in the right flank. When the tumor volume was about 150 mm^3, the mice were intraperitoneally injected once a day with vehicle (control group, $n = 7$) or DPT at 5 mg/kg ($n = 7$) in the volume of 50 μL for consecutive 12 days. A slide caliper was used to measure the tumor length (A) and width (B) and then the tumor volume was calculated according to tumor volume $= 0.5 \times A \times B^2$. When the therapy was terminated on day 12, the animals were euthanized by cervical dislocation, and tumor tissues were removed and frozen immediately in liquid nitrogen.

Measurement of NADPH oxidase activity

A chemiluminescence assay kit produced by Genmed Scientifics (Arlington, MA) was used to assay NADPH oxidase activity as described by us previously [21]. The results were expressed as the ratio of relative light unit (RLU) to the control group.

Assay of NAD^+, ROS, and H_2O_2

ROS probe DCFH-DA and H_2O_2 assay kit were both from Beyotime Biotechnology Company (China) and used as reported previously by us [5, 21]. The ROS levels were expressed as arbitrary unit/mg protein, then as the percentage of control. H_2O_2 level was expressed as a ratio to the concentration of the control cells.

NAD^+ was assayed with a NAD^+/NADH assay kit (Beyotime Biotechnology, China) as described in manufacture's protocol. In brief, NAD^+/NADH extraction buffer was added into collected cells or tumor tissue to make them lysis. For measurement of total NAD^+/NADH level, 20 μL lysis solution was transferred into a 96 wells plate, incubated with 90 μL alcohol dehydrogenase for 10 min, followed by 10 μL chromogenic solution for 30 min. The acquired absorbance value at wavelength 450 nm by a microplate reader was used to calculate the total level of NAD^+/NADH following calibration to a standard concentration curve. For

measurement of NADH level, the lysis solution needed to be heated at 60 °C for 30 min followed by incubation with dehydrogenase and chromogenic solution. The amount of NAD^+ was derived by subtracting NADH from total NAD^+/NADH and expressed as a ratio to control group.

Western blotting

Western blotting was conducted as reported previously by us [21]. In brief, cytoplasmic and nuclear fractions were obtained by centrifuging the homogenates at 1000 × *g* for 10 min. After SDS electrophoresis and transfer to PVDF membranes, the membranes were blocked and then incubated overnight at 4 °C with primary antibodies. A chemi-luminescence developer (ChemiScope 5300, Clinx Science Instrument Company, Shanghai) was used to visualize the target protein bands.

Co-immunoprecipitation

Co-immunoprecipitation was performed as described by us previously [23].

Statistical analyses

The obtained data were expressed as mean ± SD. One-way ANOVA was used to make statistical comparisons. *P* values of less than 0.05 were considered to be statistically significant.

RESULTS

SIRT1 activation boosted DPT-induced glioma cell parthanatos

To test whether SIRT1 is activated in the presence of DPT, U87, U251, and U118 cells were treated with DPT at 150 nmol/L and 450 nmol/L as reported previously by us [5]. Then, the nuclear levels of SIRT1 and phospho-SIRT1 (Ser27) were examined by Western blotting after the nuclear fractions were isolated by centrifugation. Compared with those in control cells, SIRT1 and phospho-SIRT (Ser27) were both obviously upregulated, but acetyl-p53 was downregulated by DPT in a time- and dosage-dependent manner (Fig. 1a–c). Considering that SIRT1 activity is upregulated after being phosphorylated at Ser27 and p53 deacetylation is dependent on SIRT1 activation [8, 15], these data indicated DPT triggered SIRT1 activation in glioma cells.

To clarify the role of activated SIRT in DPT-induced glioma cell death, U87 and U251 cells were treated with SIRT1 inhibitor EX527 at 200 μmol/L or SIRT1 activator SRT2183 at 10 μmol/L for 1 h and then incubated with 450 nmol/L DPT for 24 h. Although SRT2183 alone mildly upregulated and EX527 alone slightly downregulated the protein levels of SIRT1 and phospho-SIRT (Ser27) (Fig. 1b, c), LDH release assay showed no glioma cell was induced to die by SRT2183 or EX527 at indicated concentration (Fig. 1d). In contrast, SRT2183 aggravated, but EX527 suppressed DPT-induced glioma cell death (Fig. 1d). Light microscopy showed as well DPT-treated cells were morphologically shrunken and round in comparison with control ones, which became more apparent in the presence of SRT2183, but suppressed by EX527 (Fig. 1e). Moreover, Western blotting revealed SRT2183 enhanced, whereas EX527 inhibited DPT-induced increases of SIRT1 and phospho-SIRT1 (Ser27) and decrease of acetyl-p53 (Fig. 1b and c). Then, we found silence of SIRT1 with siRNA not only inhibited DPT-triggered upregulation of SIRT1 and phospho-SIRT1 (Ser27), but also obviously prevented acetyl-p53 downregulation and glioma cell death (Fig. 1f and g). These indicated SIRT1 activation contributed to DPT-induced glioma cell death (Fig. 1g).

Notably, DPT-induced upregulation of PARP1 and PAR were both found to be strengthened by SRT2183 (Fig. 1b), but suppressed by EX527 or silence of SIRT1 with siRNA (Fig. 1c, d). Considering that PAR generation depends on PARP1 activation [1], these suggested activated SIRT1 contributed to DPT-induced PARP1 expression and activation.

SIRT1 activation enhanced DPT-induced DNA DSBs and PARP1 acetylation

To elucidate why activated SIRT1 could promote PARP1 activation, we examined the effect of SIRT1 activation on DNA DSBs, which is a canonical pathway leading to PARP1 activation [8]. Neutral comet assay, a sensitive method to detect DNA DSBs, showed the cells treated with 450 nmol/L DPT for 24 h displayed long comet tails, which was inhibited by EX527, but aggravated by SRT2183 (Fig. 2a). Statistical analysis also verified EX527 inhibited, but SRT2183 strengthened DPT-induced increases in the cells with comet tails and improvement of DNA content within comet tails (Fig. 2a–c). These indicated SIRT1 activation contributed to DPT-induced DNA DSBs.

Confocal microscopy showed as well that DPT-induced nuclear accumulation of γ-H2AX (phosphos-H2AX at Ser139), molecular marker of DNA DSBs, was enhanced by SRT2183, whereas weakened by EX527 (Fig. 2d). Consistently, Western blotting proved SRT2183 reinforced, whereas EX527 weakened DPT-induced upregulation of γ-H2AX, as well as the increase of phospho-ATM which accounts for γ-H2AX generation after the occurrence of DNA DSBs (Fig. 2e and f). Therefore, these results further verified activated SIRT1 aggravated DPT-induced DNA DSBs.

Because PARP1 activity is increased after being acetylated [8], we immunoprecipitated PARP1 with its antibody and examined its acetylated level by Western blotting. In comparison with control cells, PARP1 acetylation was significantly improved by DPT in a time-dependent manner (Fig. 2g). Pretreatment with SRT2183 strengthened, but EX577 suppressed DPT-induced PARP1 acetylation (Fig. 2h). These indicated that SIRT1 activation promoted DPT-induced PARP1 acetylation.

SIRT1 activation reinforced DPT-induced NOX2 activation

Given that oxidative stress featured by ROS accumulation is a primary factor leading to DNA DSBs-dependent PARP1 activation [24], we examined the effect of DPT treatment on intracellular ROS levels by incubating U87 and U251 cells with ROS probe DCFH-DA. Fluorescence microscopy showed that the cells treated with 450 nmol/L DPT for 24 h presented brighter green fluorescence than control cells (Fig. 3a), which was also verified by statistically analyzing the fluorescence intensity (Fig. 3b). These indicated that DPT treatment improved ROS levels in glioma cells.

Because ROS could be generated from activated NADPH oxidase [25], we tested whether NADPH oxidase was involved in regulating DPT-induced ROS accumulation. It was found the activity of NADPH oxidase was significantly higher in DPT-treated cells than that in control cells (Fig. 3c). Then, Western blotting revealed the protein level of NOX2, a member of NADPH oxidase family [26], was time-dependently upregulated by DPT (Fig. 3d). To clarify the role of NOX2 in DPT-induced ROS accumulation and glioma cell death, the cells were treated with NOX2 inhibitor GSK2795039 at 5 μmol/L for 1 h and then incubated with DPT. We found GSK2795039 not only significantly inhibited DPT-induced increase in NADPH oxidase activity but also ROS accumulation (Fig. 3b, c), but also attenuated DPT-induced upregulation of phospho-ATM, γ-H2AX, PARP1, and PAR (Fig. 3e). Consistently, the glioma cell death was also rescued by GSK2795039 (Fig. 3f). Similar results could be found by knocking down NOX2 with siRNA (Fig. 3g–i). Therefore, these indicated that NOX2 contributed to DPT-induced PARP1 activation by promoting ROS-dependent DNA DSBs.

In contrast, pretreatment with SRT2183 strengthened, but EX527 suppressed DPT-induced ROS accumulation, increase in NADPH oxidase activity, and upregulation of NOX2 expression (Fig. 3b, c, j and k). Furthermore, the downregulation of phospho-AKT at Ser473 caused by DPT was also exacerbated by SRT2183, but reversed by EX527 (Fig. 3j and k). Because activated AKT acts as an interior inhibitor to suppress NOX2 expression and activation

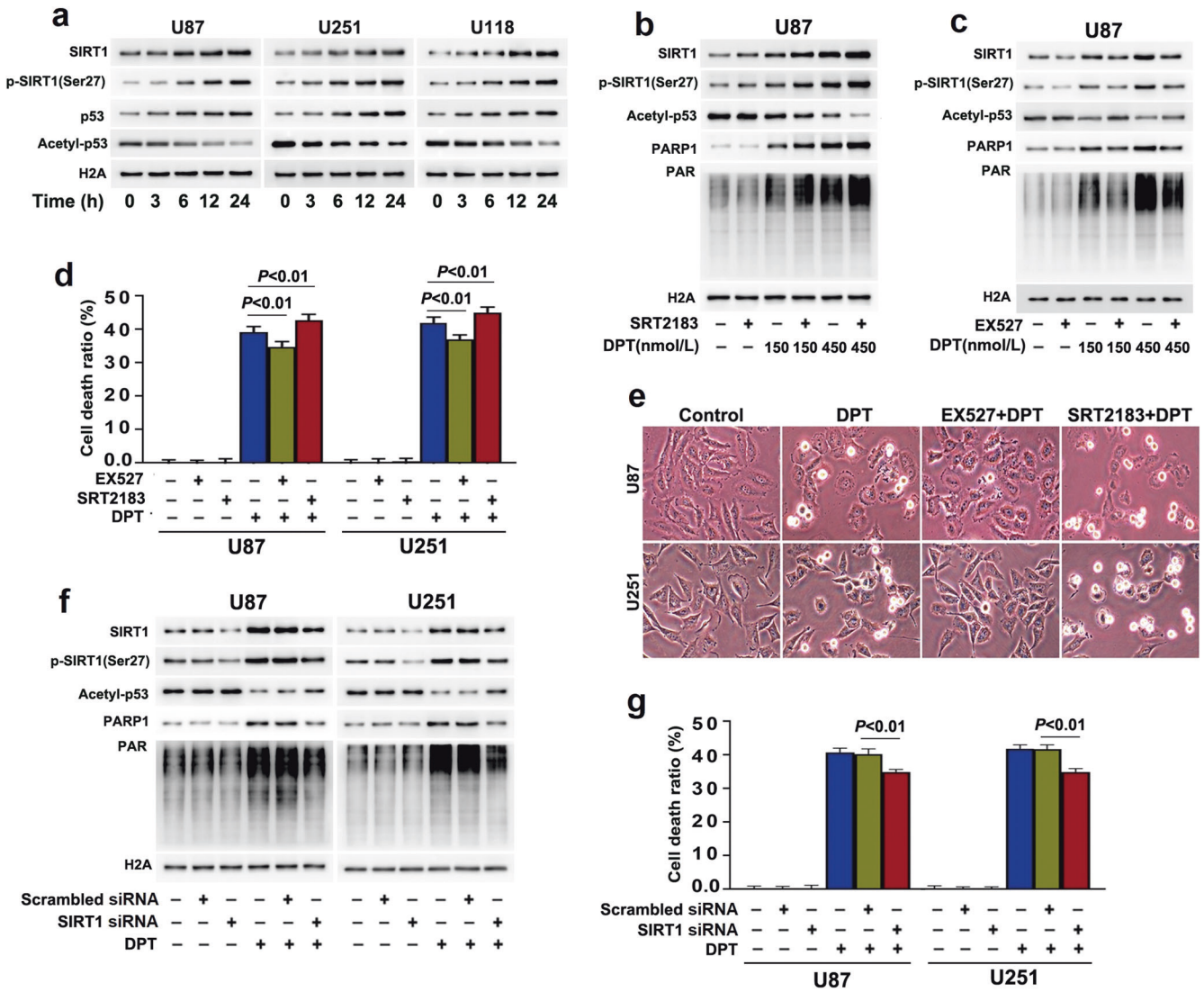

Fig. 1 SIRT1 activation boosted DPT-induced glioma cell parthanatos. a Western blotting showed that treatment with DPT at 450 nmol/L induced time-dependent upregulation of SIRT1 and phospho-SIRT at Ser27 and downregulation of acetyl-p53 in U87, U251, and U118 cells. **b** Activation of SIRT1 with 10 μmol/L SRT2183 reinforced DPT-induced downregulation of acetyl-p53 and upregulation of PARP1 and PAR. **c** Inhibition of SIRT1 with 200 μmol/L EX527 suppressed the downregulation of acetyl-p53 and the upregulation of PARP1 and PAR caused by DPT. **d** LDH release assay showed that SRT2183 aggravated, but EX527 attenuated DPT-induced glioma cell death. **e** Representative images of morphological changes in the cells treated with DPT in the presence SRT2183 or EX527 (×20). **f** Western blotting analysis proved knockdown of SIRT1 with siRNA not only prevented DPT-induced upregulation of SIRT1 and phosopho-SIRT1 at Ser27, but also alleviated DPT-triggered downregulation of acetyl-p53 and upregulation of PARP1 and PAR. **g** LDH release assay showed knockdown of SIRT1 with siRNA rescued DPT-induced glioma cell death.

[26, 27], these results suggested SIRT1 promoted DPT-induced NOX2 expression and activation via the inactivation of AKT.

SIRT1 activation reinforced DPT-induced NAT10 upregulation

To elucidate why DPT treatment reinforced PARP1 acetylation, we analyzed DPT-induced changes in p300 and NAT10, both of which are acetyltransferases and could acetylate PARP1 [28, 29]. As shown by Western blotting, NAT10 was upregulated, but p300 was downregulated by DPT in a time-dependent manner (Fig. 4a). Confocal microscopy revealed as well that the upregulated NAT10 caused by DPT was mainly located in the nucleus (Fig. 4b). Then, we found treating the cells with 50 μmol/L remodelin, a specific inhibitor of NAT10 inhibitor, significantly inhibited DPT-induced upregulation of PARP1 and PAR, as well as prevented NAT10 upregulation (Fig. 4c). Moreover, the glioma cell death caused by DPT was also attenuated in the presence of remodelin (Fig. 4d). Consistently, the upregulated PARP1 and PAR and the glioma cell death caused by DPT were all suppressed when NAT10 was knocked down with siRNA (Fig. 4e and f). These suggested NAT10 regulated DPT-induced glioma cell death via promoting PARP1 expression and activation.

To address the role of NAT10 in DPT-induced PARP1 acetylation, immunoprecipitation was used to pull down NAT10. Western blotting showed that PARP1 was co-immunoprecipitated when NAT10 was immunoprecipitated by its antibody (Fig. 4g). Although the co-immunoprecipitated PARP1 was at higher level in DPT-treated cells than that in control ones, it was obviously inhibited by treating the cells with remodelin (Fig. 4g). This indicated that DPT treatment strengthened the interaction between NAT10 and PARP1. Then, PARP1 was immunoprecipitated with its antibody and its acetylated level was assayed by Western blotting. We found DPT-induced upregulation in acetylated PARP1 was also apparently inhibited by remodelin (Fig. 4h). These indicated that NAT10 contributed to DPT-induced PARP1 acetylation.

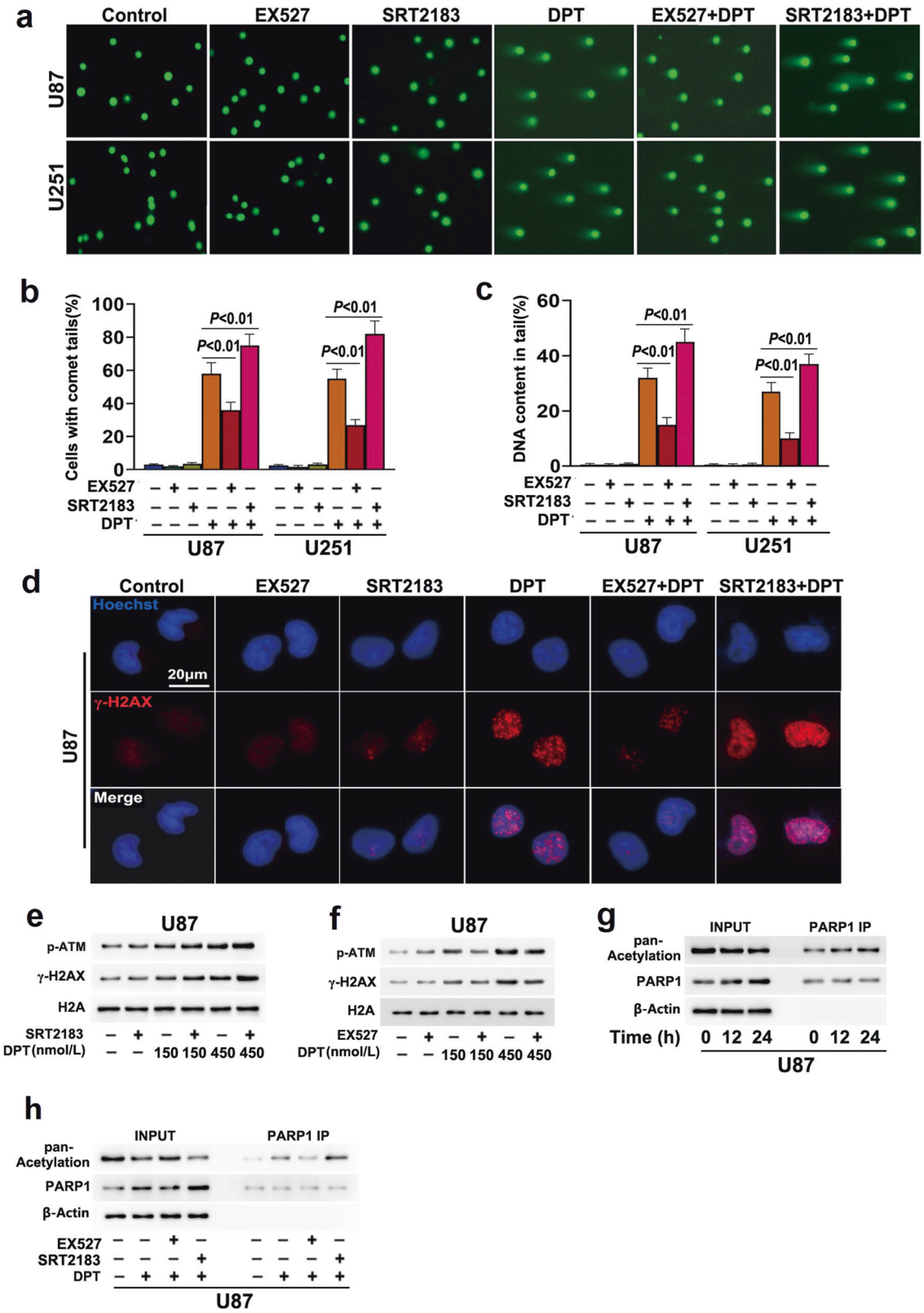

Fig. 2 SIRT1 activation enhanced DPT-induced DNA DSBs and PARP1 acetylation. a Neutral comet assay showed the cells treated with 450 nmol/L DPT for 24 h displayed comet tails, and the comet tails became more apparent when the cells were pretreated with 10 μmol/L SRT2183 for 1 h, but were inhibited by pretreatment with 200 μmol/L EX527. **b**, **c** Statistical analysis demonstrated the increased cells with comet tails and the improved DNA content within comet tails induced by DPT were strengthened by SRT2183, but suppressed by EX527. **d** Confocal microscopy revealed SRT2183 reinforced, but EX527 suppressed DPT-induced formation of γ-H2AX (phospho-H2AX at Ser139) within nuclei. **e**, **f** Western blotting proved the upregulation of γ-H2AX and phospho-ATM triggered by DPT was reinforced by SRT2183, but inhibited by EX527. **g** Western blotting analysis of the PARP1 immunoprecipitated by its antibody showed DPT upregulated PARP1 acetylation in a time-dependent manner. **h** SRT2183 aggravated, whereas EX527 alleviated DPT-induced acetylation of PARP1.

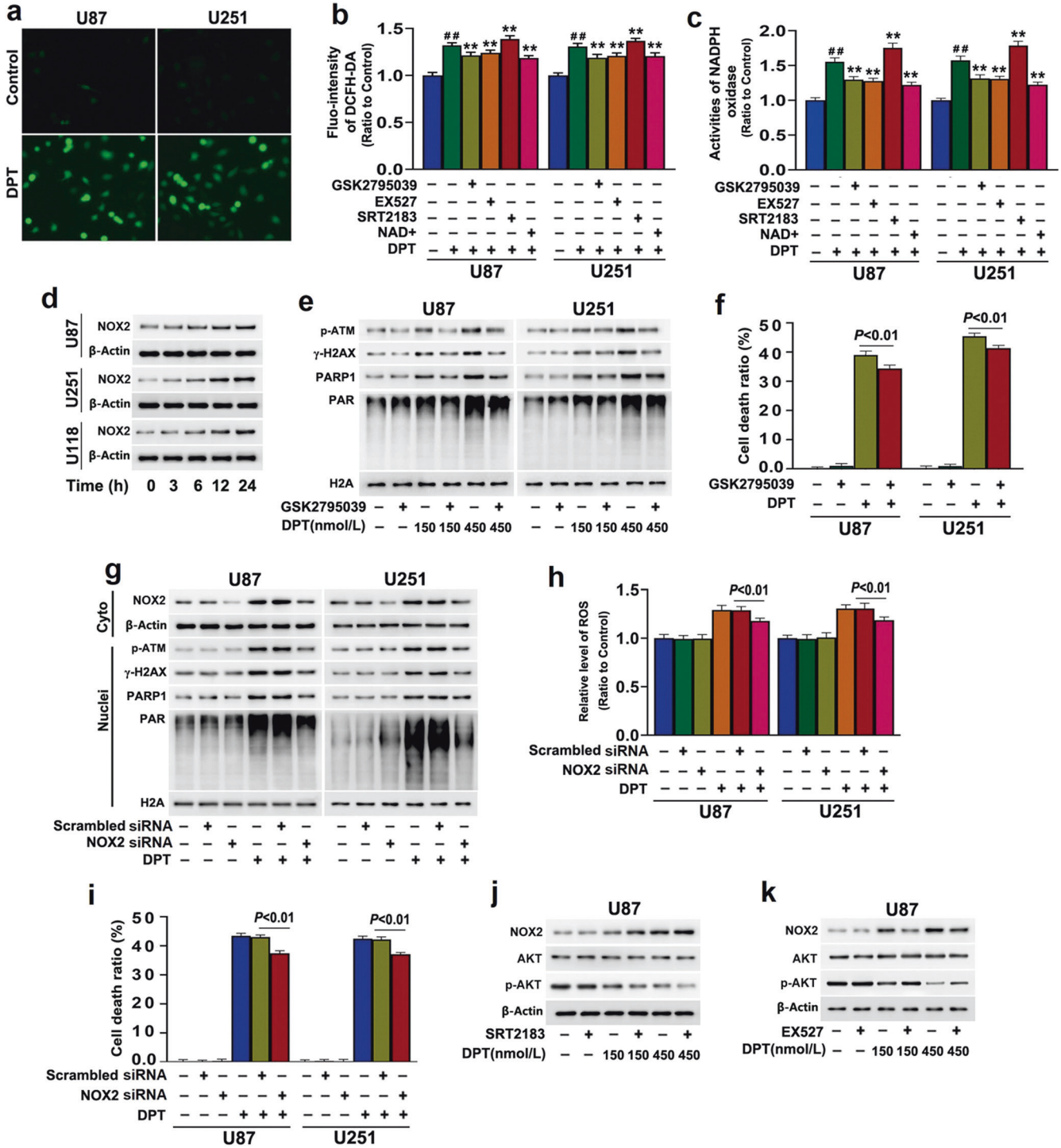

Fig. 3 SIRT1 activation reinforced DPT-induced NOX2 activation. a Representative images of the cells incubated with ROS probe DCFH-DA under fluorescence microscope showed that DPT-treated cells presented brighter green fluorescence than control cells. **b** Statistical analysis of the green fluorescence density showed DPT-induced increase of the green fluorescence was suppressed when the cells were pretreated with 5 μmol/L GSK2795039, 200 μmol/L EX527 or 2 mmol/L NAD^+, but reinforced by 10 μmol/L SRT2183. **c** NADPH oxidase activity assay showed the upregulated NADPH oxidase activity induced by DTP was inhibited by GSK2795039, EX527, or NAD^+, but aggravated by SRT2183. **d** Western blotting showed DPT induced time-dependent upregulation of NOX2 in U87, U251, and U118 cells. **e** Western blotting proved pretreatment with NOX2 inhibitor GSK2795039 obviously prevented DPT-induced upregulation of phospho-ATM, γ-H2AX, PARP1 and PAR. **f** LDH release assay showed GSK2795039 significantly rescued the glioma cell death caused by DPT. **g** Western blotting revealed knockdown of NOX2 with siRNA obviously prevented DPT-induced upregulation of phospho-ATM, γ-H2AX, PARP1 and PAR. **h** Knockdown of NOX2 with siRNA prevented DPT-induced accumulation of ROS. **i** LDH release assay showed NOX2 knockdown with SiRNA prevented the glioma cell death caused by DPT. **j**, **k** SRT2183 reinforced, but EX527 inhibited DPT-induced upregulation of NOX2 and downregulation of phospho-AKT. $^{\#\#}P < 0.01$ versus control group; $^{**}P < 0.01$ versus single DPT group.

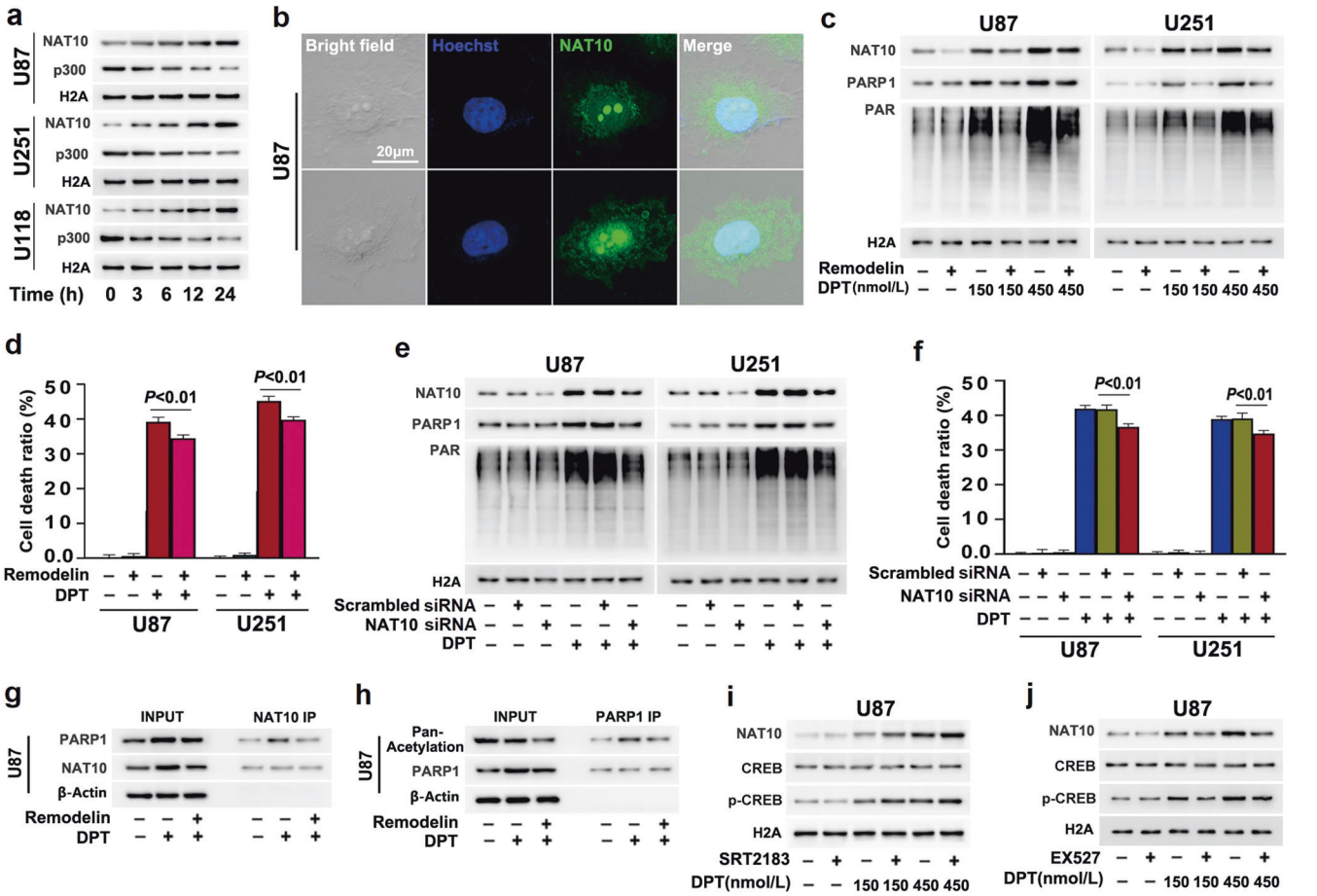

Fig. 4 SIRT1 activation reinforced DPT-induced NAT10 upregulation. **a** Western blotting showed DPT induced time-dependent upregulation of NAT10, but downregulation of p300. **b** Representative images of confocal microcopy showed the upregulated NAT10 caused by DPT was located within nucleus. **c** Western blotting proved that pretreatment with remodelin at 50 μmol/L for 1 h obviously inhibited DPT-induced upregulation of NAT10, PARP1 and PAR. **d** LDH release assay showed the glioma cell death caused by DPT was significantly rescued by remodelin. **e** Western blotting demonstrated knockdown of NAT10 with SiRNA apparently prevented DPT-induced upregulation of NAT10, but also inhibited the upregulation of PARP1 and PAR. **f** LDH release assay revealed knockdown of NAT10 with siRNA rescued DPT-induced glioma cell death. **g** Immunoprecipitation of NAT10 with its antibody showed that the increased co-immunoprecipitation of PARP1 caused by DPT was inhibited by remodelin. **h** Western blotting analysis of the PARP1 immunoprecipitated by its antibody proved DPT-induced PARP1 acetylation was suppressed by remodelin. **i**, **j** Western blotting showed SRT2183 strengthened, but EX527 suppressed DPT-induced upregulation of NAT10 and phospho-CREB.

Furthermore, we found that DPT-induced upregulation of NAT10 and phospho-CREB at Ser133 were both strengthened by SRT2183 (Fig. 4i), but suppressed by EX527 (Fig. 4j). Given that CREB phosphorylation could upregulate NAT10 expression [30], our data indicated that SIRT1 promoted DPT-induced upregulation of NAT10 via regulation of CREB phosphorylation.

NAD^+ depletion contributed to DPT-induced upregulation of NAT10 and NOX2

Because SIRT1 activation could lead to NAD^+ depletion [18], we examined the effect of DPT treatment on intracellular NAD^+ levels. It was found treatment with DPT at 450 nmol/L resulted in time-dependent depletion of NAD^+ in glioma cells (Fig. 5a). To address the role of NAD^+ depletion in DPT-induced glioma cell death, the cells were pretreated 1 h with exterior NAD^+ at indicated dosages or 10 μmol/L FK866 which could inhibit NAD^+ synthesis from nicotinamide via salvage pathway by targeting NAMPT1. We found supplement of NAD^+ significantly rescued DPT-induced cell death, and the rescue became more apparent when NAD^+ dosage was increased from 0.5 to 2.0 mmol/L (Fig. 5b). In contrast, the cell death was exacerbated when NAD^+ level was further decreased by FK866 (Fig. 5c and d). Then, Western blotting and co-immunoprecipitation revealed that supplement of NAD^+ inhibited, but FK866 reinforced DPT-induced PARP1 expression, PAR generation, and PARP1 acetylation (Fig. 5e–g). These indicated NAD^+ depletion contributed to DPT-induced glioma cell death by improving PARP1 activation.

Then, we examined the role of NAD^+ depletion in DPT-induced changes in NOX2 and NAT10. We found supplement of NAD^+ inhibited, but FK866 strengthened DPT-induced ROS (Fig. 3b), increase in NADPH oxidase activity (Fig. 3c), upregulation of NOX2 and NAT10 expression (Fig. 5e and f) and enhancement in the interaction between NAT10 and PARP1 (Fig. 5g). Moreover, DPT-induced downregulation of phospho-AKT and upregulation of phospho-CREB were also prevented by NAD^+, but aggravated by FK866 (Fig. 5e and f). Notably, the NAD^+ decrease caused by DPT was exacerbated by SRT2183, but attenuated by EX527 (Fig. 5h). Taken together, these results indicated SIRT1-dependent NAD^+ depletion contributed to DPT-induced PARP1 activation via regulating NOX2 activation and NAT10 expression

To further verify that NAD^+ depletion regulates NOX2 activation and NAT10 expression, U87 and U251 cells were treated with 500 μmol/L FK866 for indicated time. We found FK866 not only decreased NAD^+ level at 12 h and 24 h after incubation (Fig. 5i),

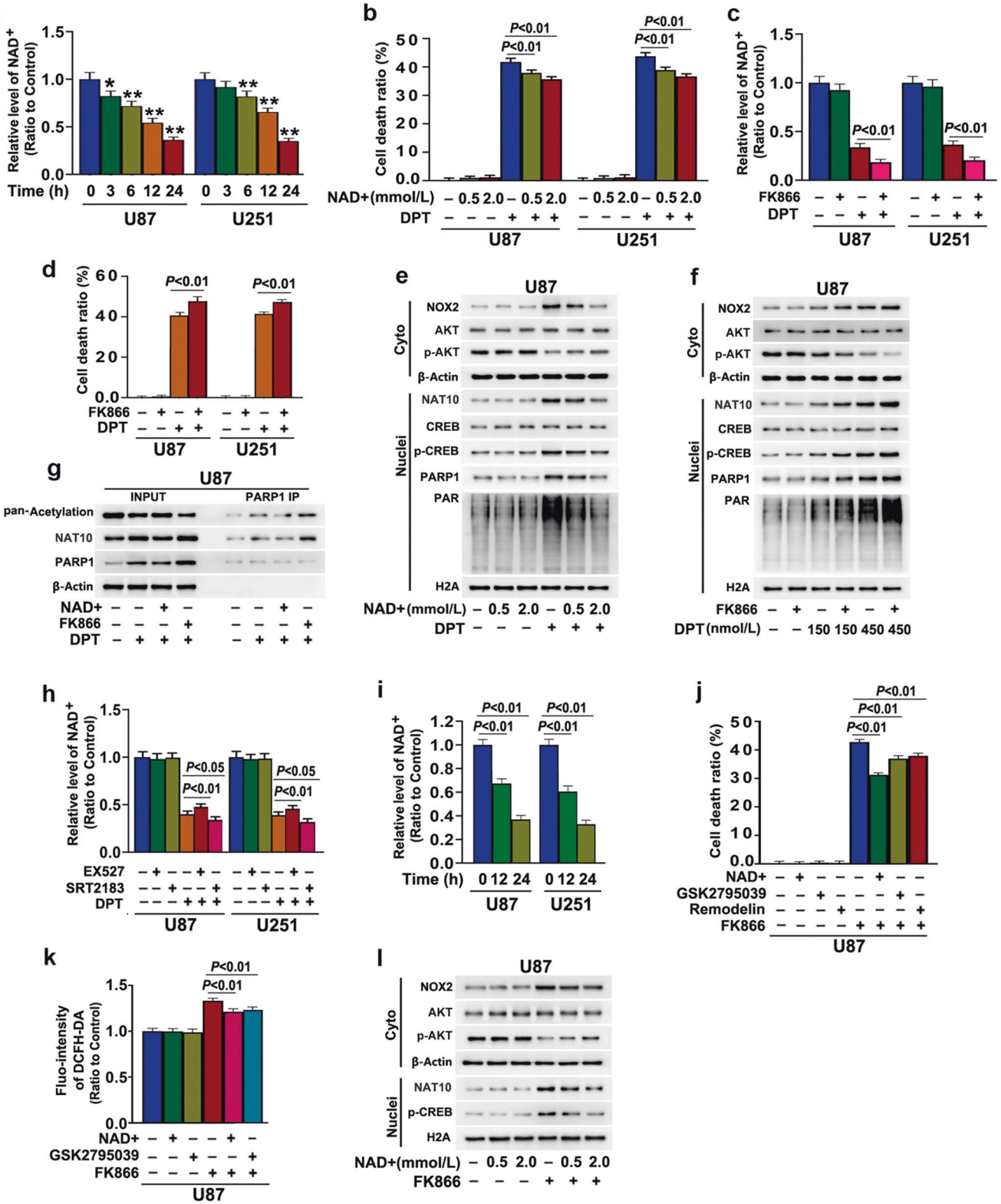

but also triggered glioma cell death, ROS accumulation, phospho-AKT downregulation, and upregulation of phospho-CREB, NOX2 and NAT10 (Fig. 5j–l). In contrast, FK866-triggered cell death was significantly prevented by treating the cells with 50 μmol/L NAT10 inhibitor remodelin or 5 μmol/L NOX2 inhibitor GSK2795039 (Fig. 5j). Moreover, the increased ROS was also inhibited by GSK2795039 (Fig. 5k). These indicated that NOX2 and NAT10 contributed to FK866-induced glioma cell death. Notably, supplement of exterior NAD^+ not only inhibited FK866-induced cell death and ROS accumulation, but also alleviated the downregulation of phospho-AKT, and the upregulation of phospho-CREB, NOX2 and NAT10 in a dosage-dependent manner (Fig. 5l).

Fig. 5 NAD^+ depletion contributed to DPT-induced upregulation of NAT10 and NOX2. a Treatment with 450 nmol/L DPT resulted in time-dependent depletion of NAD^+. **b** LDH release assay showed supplement of exterior NAD^+ at indicated concentration inhibited DPT-induced glioma cell death in a dosage-dependent manner. **c** Pretreatment of 100 μmol/L FK866 for 1 h significantly aggravated DPT-induced depletion of NAD^+. **d** LDH release assay showed FK866 exacerbated the glioma cell death caused by DPT. **e** Western blotting proved supplement of exterior NAD^+ dosage-dependently alleviated DPT-induced downregulation of phospho-AKT and upregulation of NOX2, NAT10, phospho-CREB, PARP1, and PAR. **f** Western blotting demonstrated FK866 aggravated DPT-induced downregulation of phospho-AKT and upregulation of NOX2, NAT10, phospho-CREB, PARP1, and PAR. **g** Western blotting analysis of the immunoprecipitated PARP1 with its antibody proved the upregulated PARP1 acetylation and the increased co-immunoprecipitation of NAT10 induced by DPT were both suppressed by supplement of exterior NAD^+, but aggravated by FK866. **h** Pretreatment with SRT2183 exacerbated, but EX527 alleviated DPT-induced depletion of NAD^+. **i** Treatment with 500 μmol/L FK866 resulted in time-dependent depletion of NAD^+. **j** LDH release assay showed the glioma cell death caused by 500 μmol/L FK866 was significantly attenuated by pretreatment with NAD^+, GSK2795039 or remodelin. **k** NAD^+ and GSK2795039 respectively inhibited FK866-induced accumulation of ROS. **l** Western blotting revealed that supplement of exterior of NAD^+ dosage-dependently prevented FK866-induced downregulation of phospho-AKT and upregulation of NOX2, NAT10 and phospho-CREB. $^*P < 0.05$, $^{**}P < 0.01$ versus control group.

Taken together, these data indicated that NAD^+ depletion plays a crucial role in regulating NAT10 expression and NOX2 activation in glioma cells.

JNK regulated DPT-induced SIRT1 activation

Given that SIRT1 is activated when phosphorylated at Ser27 by JNK [15], we tested whether JNK was activated in the presence of DPT. Although no changes could be found in the level of JNK between DPT-treated cells and control cells, phospho-JNK was upregulated by DPT in a time-dependent manner (Fig. 6a), indicating DPT treatment resulted in JNK activation. In contrast, the cell death caused by DPT, as well as phospho-JNK upregulation, was obviously suppressed by treating the cells with 15 μmol/L SP600125, a specific inhibitor of JNK (Fig. 6b and c). Similar results were found by silence of JNK with siRNA (Fig. 6d and e). Moreover, DPT-induced upregulation of PARP1 expression and PAR generation were also effectively inhibited by SP600125 or silence of JNK (Fig. 6c and d). These data suggested that activated JNK contributed to DPT-induced glioma cell parthanatos.

Notably, it was shown that either SP600125 or knockdown of SIRT1 with siRNA significantly alleviated DPT-induced upregulation of phospho-SIRT1(Ser27) (Fig. 6c and d). Furthermore, DPT-induced SIRT1-dependent acetyl-p53 downregulation, NAD^+ depletion, and upregulation of NOX2 and NAT10 were all correspondingly inhibited (Fig. 6c, d, f and g). These indicated that JNK accounted for DPT-induced activation of SIRT1.

SIRT1-dependent NAD^+ depletion reversely promoted DPT-induced JNK activation

Because ASK1 is an upstream signaling regulating JNK activation and could be activated by ROS [31], we evaluated the effect of DPT on ASK1 activation. As revealed by Western blotting, DPT triggered dosage-dependent upregulation of ASK1 and phospho-ASK1 at T845, which was obviously inhibited by NOX2 inhibitor GSK2795039 or when NOX2 was knocked down with siRNA (Fig. 7a and b). Correspondingly, the upregulated phospho-JNK caused by DPT was suppressed as well. These suggested NOX2 contributed to DPT-induced activation of ASK1/JNK pathway.

Because NOX2 activation induced by DPT depended on SIRT1-regulated NAD^+ depletion, we evaluated the role of NAD^+ in DPT-induced activation of ASK/JNK signaling. It was shown that supplement of exterior NAD^+ suppressed, but FK866 aggravated DPT-induced upregulation of ASK1, phospho-ASK1 at T845 and phospho-JNK (Fig. 7c and d). Similar results could be found when the cells were pretreated with SIRT1 inhibitor EX527 or activator SRT2183(Fig. 7e and f). Thus, activated SIRT1 reversely promoted DPT-induced activation of ASK1/JNK signals via triggering NAD^+ depletion-dependent activation of NOX2.

DPT induced activation of PARP1 and SIRT1 in vivo

To verify that SIRT1 and PARP1 could be activated simultaneously by DPT in vivo, we established xenografted glioma model by injecting subcutaneously U87 cells into the flank of mice, and then the mice were treated once a day with DPT for consecutive twelve days. Twelve days treatment with DPT made tumor volume and weight being significantly less than that in control group (Fig. 8a). These indicated that DPT could effectively inhibit the growth of glioma cells in vivo.

To detect whether DPT could induce PARP1 activation in vivo, Western blotting was used to analyze DPT-induced changes in PAR generation and the expressions of PARP1, γ-H2AX and phospho-ATM. Compared with control group, PAR, PARP1, γ-H2AX, and phospho-ATM were all obviously upregulated by DPT (Fig. 8b). Considering that DNA DSBs characterized by upregulation of γ-H2AX and phospho-ATM are a canonical pathway leading to PARP1 activation and activated PARP1 could generate PAR polymers, these results indicated that PARP1 could be activated by DPT in vivo. Then, we found that NOX2 expression, NADPH oxidase activity and H_2O_2 level were all upregulated, but phospho-AKT was downregulated in DPT-treated gliomas in comparison with control group (Fig. 8c–e). These indicated that DPT-induced DNA DSBs might be associated with NOX2-regulated oxidative stress.

Because phospho-CREB and NAT10 were both upregulated by DPT (Fig. 8c), we used immunoprecipitation to assay the interaction between NAT10 and PARP1. When NAT10 was immunoprecipitated by its antibody, the co-immunoprecipitated PARP1 was at higher level in DPT-treated group than that in control group (Fig. 8f). Moreover, the acetylated level of PARP1 was also obviously increased by DPT (Fig. 8g). Considering that PARP1 could be acetylated by NAT10 [29], these indicated NAT10 regulated the PARP1 activation caused by DPT.

Furthermore, phosho-ASK1 and phospho-JNK were both upregulated in DPT-treated group when compared with control group (Fig. 8c), indicating that DPT treatment activated ASK1/JNK pathway. Additionally, we found the protein levels of SIRT1 and phospho-SIRT1 at Ser27 were both increased, but acetyl-p53 and NAD^+ levels were both decreased by DPT(Fig. 8c and h). Given that SIRT1 is activated when being phosphorylated by JNK at Ser27 and activated SIRT1 could deacetylate p53 by consuming NAD^+ [8, 15], our data indicated JNK contributed to DPT-induced SIRT activation in vivo.

DISCUSSION

In summary, we demonstrated in this study that PARP1 and SIRT1 were both activated by DPT in glioma cells in vitro and in vivo. Pharmacological activation of SIRT1 with SRT2183 promoted, but inhibition of SIRT1 with EX527 or genetic knockdown of SIRT1 with SiRNA attenuated DPT-induced PARP1 activation and glioma cell death. Mechanistically, SIRT1 activation resulted in decrease of intracellular NAD^+. Further decrease of NAD^+ with FK866 aggravated, but supplement of exterior NAD^+ prevented DPT-induced PARP1 activation, as well as glioma cell death. Then, we

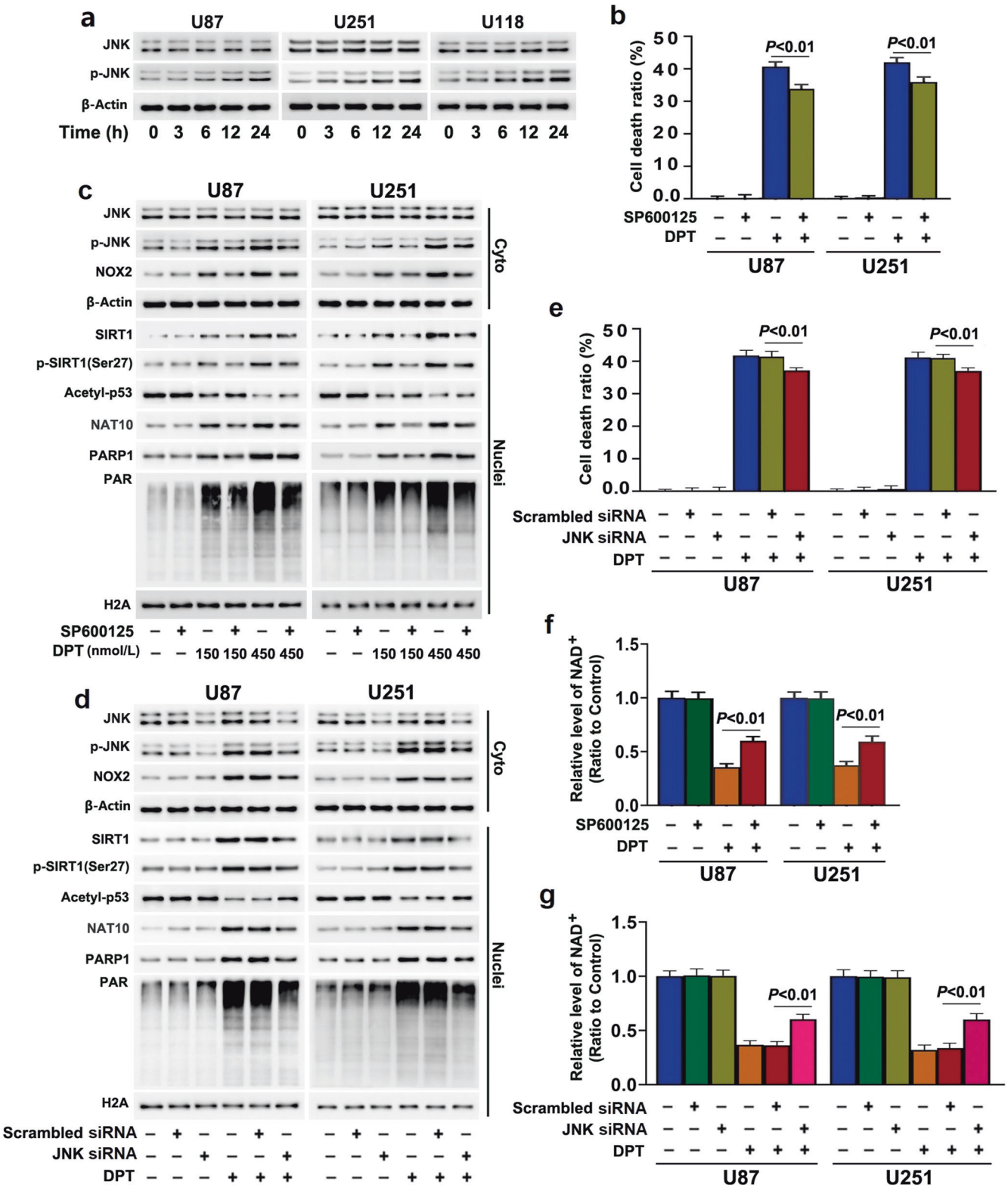

Fig. 6 JNK regulated DPT-induced SIRT1 activation. a DPT induced time-dependent upregulation of phospho-JNK in U87, U251, and U118 cells. **b** LDH release assay showed pretreatment with SP600125 rescued DPT-induced glioma cell death. **c** Western blotting revealed SP600125 apparently inhibited DPT-induced downregulation of acetyl-p53 and upregulation of phospho-JNK, NOX2, NAT10, SIRT1, phospho-SIRT1 at Ser27, PARP1 and PAR. **d** Western blotting proved that knockdown of JNK with siRNA not only prevented DPT-induced phospho-JNK upregulation, but also alleviated the downregulation of acetyl-p53 and upregulation of NOX2, NAT10, SIRT1, phospho-SIRT1 at Ser27, PARP1 and PAR. **e** LDH release assay showed that knockdown of JNK with siRNA rescued DPT-induced glioma cell death. **f** Pretreatment with SP600125 obviously reversed DPT-induced NAD^+ depletion. **g** Knockdown of JNK with siRNA significantly prevented NAD^+ depletion caused by DPT.

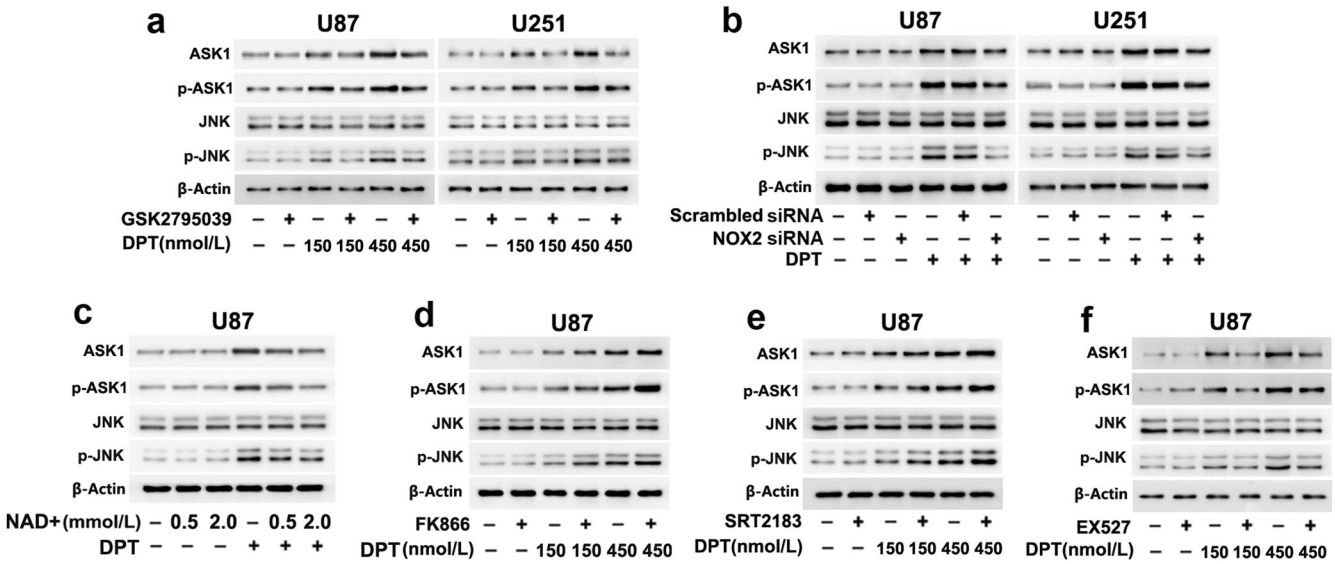

Fig. 7 SIRT1-dependent NAD^+ depletion reversely promoted DPT-induced JNK activation. a Western blotting proved DPT-induced upregulation of phospho-ASK1 and phospho-JNK was obviously inhibited by GSK2795039. **b** Knockdown of NOX2 with SiRNA prevented DPT-induced upregulation of phospho-ASK1 and phospho-JNK. **c** Supplement of exterior NAD^+ dosage-dependently suppressed DPT-induced upregulation of phospho-ASK1 and phospho-JNK. **d** FK866 reinforced DPT-induced increases of phospho-ASK1 and phospho-JNK. **e**, **f** SRT2183 aggravated, but EX527 inhibited DPT-induced upregulation of phospho-ASK1 and phospho-JNK.

found NAD^+ depletion enhanced DPT-induced PARP1 activation via two pathways, one was aggravating ROS-dependent DNA DSBs by upregulation of NOX2 and the other was reinforcing PARP1 acetylation via increasing the expression of NAT10. We also found that SIRT1 activation depended on JNK, which phosphorylated SIRT1 at Ser27. Furthermore, activated SIRT1 reversely aggravated JNK activation via upregulating ROS-related ASK1 signaling. Taken together, our data suggested that SIRT1 activated by JNK contributed to DPT-induced parthanatos in glioma cell via initiation of NAD^+ depletion-dependent upregulation of NOX2 and NAT10 (Fig. 9).

SIRT1 is demonstrated to promote cancer cells' apoptotic, autophagic, and pyroptotic death [11–13], but it often acts as a negative regulator of parthanatos by deacetylation of PARP1. As well as deacetylation of its downstream signals, SIRT1 also regulates cellular destiny by depletion of NAD^+, which is a molecule with the ability to transport across plasma membranes of cells [32]. NAD^+ depletion could initiate different modes of programmed death in multiple types of cells such as apoptosis in breast cancer cells, autophagic death in glioma cells, and necroptosis in macrophages [33–35]. However, the role of NAD^+ in parthanatos seems to be in dispute. Fueling PARP1 with NAD^+ was found to exacerbate skin cell parthanatos induced by inflammation [36], but increasing studies have shown that NAD^+ decrease contributes to PARP-1-mediated cell death. Repletion of NAD^+ not only decreased neuronal and glial parthanatos induced by cerebral ischemia, but also inhibited SH-SY5Y cell parthanatos caused by ropivacaine [24, 37]. Further study revealed NAD^+ depletion by activated PARP1 could trigger BNIP3-mediated mitochondrial damage or block glycolysis [38, 39]. Despite we reported previously that DPT induced parthanatos in glioma cells [5], in which the roles of SIRT1 and NAD^+ were both unknown. In this study, we found that PARP1 expression and PAR generation were both reinforced when DPT-induced NAD^+ depletion was aggravated by FK866, but inhibited by supplement of exterior NAD^+. This indicated NAD^+ depletion could promote PARP1 expression and activation. Notably, we found DPT-induced NAD^+ depletion was dependent on SIRT activation. Therefore, activated SIRT1 exacerbated DPT-induced glioma cell parthanatos by upregulating PARP1 expression and activation.

DNA DSBs due to oxidative stress featured by abnormal increases of intracellular ROS are regarded as a primary factor leading to PARP1 over-activation [8]. In this study, we found NOX2 strengthened DPT-induced PARP1 activation by mediating ROS-dependent DNA DSBs. Although activated SIRT1 contributed to etoposide-induced generation of ROS [39], its underlying mechanism remains unclear. In this study, we found that SIRT1 activation not only resulted in AKT de-phosphorylation, but also promoted NOX2 expression and activation. Consistently, resveratrol was found to inactivate AKT in hepatocellular carcinoma cells via activating SIRT1 [40, 41]. AKT inactivation-regulated ROS generation was shown to be dependent on NOX2 expression and activation. It was reported that hypoxia and reoxygenation induced NOX2-dependent generation of ROS in cardiomyocytes by inactivating AKT [26]. LPS-induced de-phosphorylation of AKT boosted NOX2 expression and ROS production in microglial cells [27]. Furthermore, AKT activation also depends on intracellular NAD^+ levels. It was shown AKT activation was enhanced when NAD^+ level was increased by over-expression of NAMPT, a key enzyme regulating NAD^+ synthesis via salvage pathway [42], but suppressed when NAMPT was inhibited with STF-118804 [43]. It was noteworthy that nicotinamide, which is not only an inhibitor of SIRT1 but also could be used for NAD^+ synthesis, obviously prevented Ultraviolet B light-induced AKT inactivation in corneal endothelial cells [44]. Thus, NAD^+ regulates AKT activation not via activation of SIRT1. Therefore, these previous studies suggest SIRT1 inhibits AKT activity by depletion of NAD^+, which increases ROS by upregulating NOX2 expression and activation. In this study, we found the downregulated phospho-AKT and activation of NOX2 caused by DPT were both aggravated when NAD^+ was further decreased by FK866, but inhibited by supplement of NAD^+. Therefore, SIRT1 contributed to DPT-induced NOX2-dependent ROS generation by depletion of NAD^+.

Besides being improved under the condition of DNA DSBs, PARP1 activity is also upregulated after being acetylated by p300 or NAT10 [28, 29]. NAT10 is a nucleolar protein containing an acetyltransferase domain and primarily accounts for acetylation of mRNA [45]. As well as Che-1, α-tubulin and MORC2, PARP1 is a target of NAT10 and could be acetylated by NAT10 at lysine 949 [46]. NAT10-regulated acetylation of PARP1 prevented its

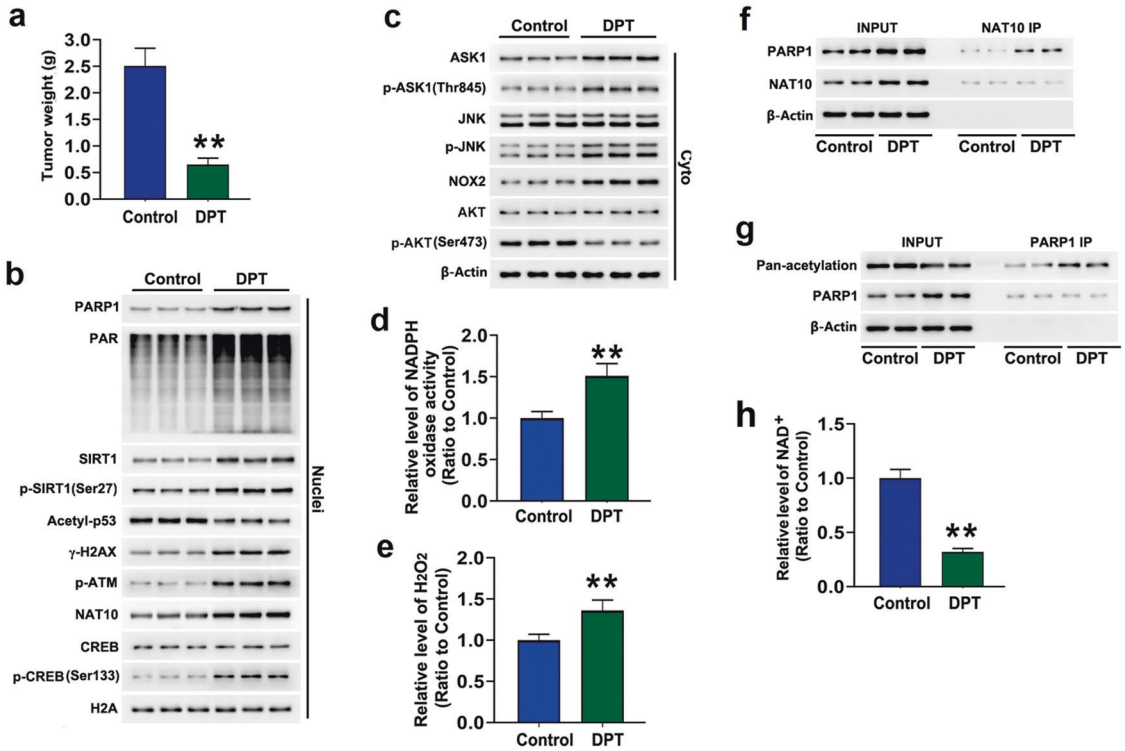

Fig. 8 DPT induced activation of PARP1 and SIRT1 in vivo. a The average tumor weight in DPT-treated group was lighter than that in control group. **b**, **c** Western blotting revealed that DPT treatment resulted in downregulation of acetyl-p53 and phospho-AKT, but upregulation of PARP1, PAR, SIRT1, phospho-SIRT1, γ-H2AX, phospho-ATM, NAT10, NOX2, phospho-CREB, phospho-ASK1, and phospho-JNK. **d** DPT treatment improved the activity of NADPH oxidase. **e** DPT treatment increased hydrogen peroxide level. **f** Western blotting analysis of the immunoprecipitated NAT10 showed that PARP1 co-immunoprecipitation was increased by DPT. **g** Western blotting analysis of the immunoprecipitated PARP1 showed PARP1 acetylation was reinforced by DPT. **h** DPT induced NAD^+ depletion in vivo. $^{**}P < 0.01$ versus control group.

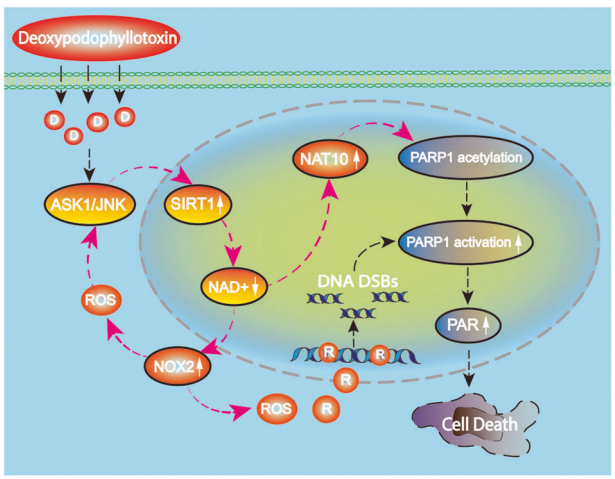

Fig. 9 Schematic diagram of activated SIRT1 regulating glioma cell parthanatos induced by DPT. DPT treatment induces JNK activation, which further activates SIRT1 by phosphorylation of Ser27. Activated SIRT1 decreased intracellular NAD^+ level, which then aggravates PARP1 activation via two pathways. One is triggering NOX2 activation to exacerbate ROS accumulation and DNA DSBs and the other is upregulation of NAT10-regulated PARP1 acetylation. Ultimately, the cytotoxic PAR polymers generated by activated PARP1 lead to cell death. Furthermore, the increased ROS reversely improves JNK phosphorylation via promotion of ASK1 activation. Thus, DPT induces positive feedback between JNK and SIRT1. Taken together, SIRT1 activated by JNK contributed to DPT-induced glioma cell parthanatos via initiation of NAD^+ depletion-dependent upregulation of NOX2 and NAT10.

ubiquitination at the same residue by E3 ubiquitin ligase CHFR and its degradation by proteasome [29]. Moreover, NAT10 overexpression could also lead to cell death. NAT10 was found to exacerbate the cardiomyocyte death caused by ischemia and reperfusion by upregulating the transcription of pro-apoptotic factor BCL2-interacting killer [47]. In this study, we found that pharmacological inhibition of NAT10 with remodelin or genetic knockdown of NAT10 with siRNA attenuated DPT-induced PARP1 acetylation and PAR generation. Thus, NAT10-regulated PARP1 acetylation contributed to DPT-induced PARP1 activation. Although NAT10 expression could be increased by genotoxic agents hydrogen peroxide and cisplatin [48], transcription factor cAMP responsive element binding protein (CREB) is an upstream signal promoting NAT10 expression. Mechanistically, CREB up-regulates NAT10 expression via inhibition of MYCT1 expression by direct binding to MYCT1 promoter [30]. Notably, CREB phosphorylation is upregulated when SIRT1 is activated or NAD^+ is decreased. SIRT1 was found to protect neurons against mutant huntingtin by activation of CREB transcriptional pathway [49]. In contrast, exogenous NAD^+ was reported to stimulate MUC2 expression via inhibition of CREB signaling pathway [50]. These indicated SIRT1 up-regulates NAT10 expression by inducing NAD^+ depletion-dependent phosphorylation of CREB. In this study, we found that inhibition of SIRT1 or supplement of NAD^+ significantly prevented DPT-triggered NAT10 expression, as well as CREB phosphorylation. Thus, SIRT1-dependent NAD^+ depletion contributed to NAT10 upregulation via upregulating CREB phosphorylation.

Although NAD^+ is regarded as the principal regulator of SIRT1 activation, the deacetylase activity of SIRT1 could also be enhanced independent of NAD^+ increase [14]. The activity of

SIRT1 is mediated by multiple types of translational modification such as S-nitrosylation, sulfhydration, and ubiquitination [51–54]. Phosphorylation-regulated SIRT1 activation has been studied extensively. Thirteen residues within SIRT1 were identified to be phosphorylated in vivo by using mass spectrometry and in vitro study revealed that the deacetylase activity of SIRT1 was decreased when SIRT1 was dephosphorylated by phosphatases even if in the presence of NAD^+ [55]. Moreover, AMPK, CK2, and JNK were upstream regulators responsible for phosphorylation of SIRT1. Although these kinases phosphorylate different sites within SIRT1, SIRT1's stability, substrate-binding affinity and deacetylase activity are all significantly improved. It was found that phosphorylation of SIRT1 by AMPK on T344 not only made it release from its endogenous inhibitor DBC1, but also improved its activity in deacetylation of p53 [56]. Phosphorylation of SIRT1 by CK2 at the conserved residues Ser 154, 649, 651, and 683 improved its deacetylation rate and substrate-binding affinity [57]. JNK promoted SIRT1 nuclear localization and increased its enzymatic activity via phosphorylation of its residues at Ser27 and Ser47 [16, 17]. Moreover, the half-life of SIRT1 was extended from <2 h to >9 h when SIRT1 is phosphorylated at serine 27 [17]. When serine 27 was substituted by alanine, the mutant form of SIRT1 exhibited lower protein stability in comparison with that of wild-type SIRT1 [15]. In this study, we found that inhibition of JNK activation with SP600125 or knockdown of JNK with siRNA obviously prevented DPT-induced SIRT1 phosphorylation at Ser27, as well as SIRT1-regulated reduction of acetyl-p53 and NAD^+ depletion. Thus, DPT induced SIRT1 activation via JNK pathway.

SIRT1 activation is regulated by JNK, but previous studies also suggest that activated SIRT1 could reversely promote JNK activation. JNK activation depends on its upstream regulator apoptosis signal-regulating kinase 1 (ASK1) whose activity is upregulated when ROS are increased. It was reported that gefitinib, an epidermal growth factor receptor inhibitor, triggered glioma cell death via causing ROS-dependent activation of ASK1/JNK pathway [58]. Moreover, we found previously that phospho-JNK was significantly upregulated in the glioma cells stressed with hydrogen peroxide which is a member of ROS [59]. Besides increasing ROS levels by activating NOX2 as demonstrated in this study, SIRT1 could also improve ROS via initiation of autophagy. This is because SIRT1 contributed to F0911-7667-induced excessive autophagy in glioma cells and autophagy was reported to improve ROS in glioma cells by causing GSH depletion-dependent accumulation of hydrogen peroxide [11, 60]. In this study, we found that SIRT1-dependnet NAD^+ depletion not only improved intracellular ROS levels, but also activated ASK1/JNK signaling. Considering that SIRT1 activation induced by DPT was dependent on JNK, we think that DPT induced a positive feedback between SIRT1 and JNK, which exacerbated glioma cell parthanatos.

In conclusion, we demonstrated in this study that PARP1 and SIRT1 were both activated by DPT in glioma cells. SIRT1-dependent NAD^+ depletion contributed to glioma cell death and PARP1 activation via promoting NOX2-dependnet DNA DSBs and reinforcing NAT10-regulated PARP1 acetylation.

ACKNOWLEDGEMENTS

This work was supported by National Natural and Science Foundation of China (81772669, 81972346 and 82173027), Scientific Research Foundation of Jilin province (20230508060RC, 20200201466JC), and Collaboration Fund of the First Hospital of Jilin University and Changchun institute of applied chemistry Chinese academy of sciences (2022YYGFZJC011).

AUTHOR CONTRIBUTIONS

This study was conceived, designed, and interpreted by PFG, SPL, and GFC. SPL, XZW, XC, ZCW, CL, SL, CH, YBW, YLW, and MHP undertook the data acquisition and analysis. MHP and GFC were responsible for the comprehensive technical support. PFG and SPL were major contributors in writing the manuscript. MHP and GFC contributed to the inspection of data and final manuscript. All authors read and approved the final manuscript.

ADDITIONAL INFORMATION

Competing interests: The authors declare no competing interests.

REFERENCES

1. Wang X, Ge P. Parthanatos in the pathogenesis of nervous system diseases. Neuroscience. 2020;449:241–50.
2. Alano CC, Garnier P, Ying W, Higashi Y, Kauppinen TM, Swanson RA. NAD^+ depletion is necessary and sufficient for poly(ADP-ribose) polymerase-1-mediated neuronal death. J Neurosci. 2010;30:2967–78.
3. Ying W. NAD^+/NADH and $NADP^+$/NADPH in cellular functions and cell death: regulation and biological consequences. Antioxid Redox Signal. 2008;10:179–206.
4. Hou WH, Chen SH, Yu X. Poly-ADP ribosylation in DNA damage response and cancer therapy. Mutat Res Rev Mutat Res. 2019;780:82–91.
5. Ma D, Lu B, Feng C, Wang C, Wang Y, Luo T, et al. Deoxypodophyllotoxin triggers parthanatos in glioma cells via induction of excessive ROS. Cancer Lett. 2016;371:194–204.
6. Paul S, Jakhar R, Bhardwaj M, Chauhan AK, Kang SC. Fumonisin B1 induces poly (ADP-ribose) (PAR) polymer-mediated cell death (parthanatos) in neuroblastoma. Food Chem Toxicol. 2021;154:112326.
7. Li D, Kou Y, Gao Y, Liu S, Yang P, Hasegawa T, et al. Oxaliplatin induces the PARP1-mediated parthanatos in oral squamous cell carcinoma by increasing production of ROS. Aging. 2021;13:4242–57.
8. Luna A, Aladjem MI, Kohn KW. SIRT1/PARP1 crosstalk: connecting DNA damage and metabolism. Genome Integr. 2013;4:6.
9. Li C, Liu Z, Yang K, Chen X, Zeng Y, Liu J, et al. miR-133b inhibits glioma cell proliferation and invasion by targeting Sirt1. Oncotarget. 2016;7:36247–54.
10. Chen H, Lin R, Zhang Z, Wei Q, Zhong Z, Huang J, et al. Sirtuin 1 knockdown inhibits glioma cell proliferation and potentiates temozolomide toxicity via facilitation of reactive oxygen species generation. Oncol Lett. 2019;17:5343–50.
11. Yao Z-Q, Zhang X, Zhen Y, He X-Y, Zhao S, Li X-F, et al. A novel small-molecule activator of Sirtuin-1 induces autophagic cell death/mitophagy as a potential therapeutic strategy in glioblastoma. Cell Death Dis. 2018;9:767.
12. Lee Y-H, Chen H-Y, Su LJ, Chueh PJ. Sirtuin 1 (SIRT1) deacetylase activity and NAD^+/NADH ratio are imperative for capsaicin-mediated programmed cell death. J Agric Food Chem. 2015;63:7361–70.
13. Zheng Z, Bian Y, Zhang Y, Ren G, Li G. Metformin activates AMPK/SIRT1/NF-kappaB pathway and induces mitochondrial dysfunction to drive caspase3/GSDME-mediated cancer cell pyroptosis. Cell Cycle. 2020;19:1089–104.
14. Gerhart-Hines Z, Dominy JE Jr., Blattler SM, Jedrychowski MP, Banks AS, Lim JH, et al. The cAMP/PKA pathway rapidly activates SIRT1 to promote fatty acid oxidation independently of changes in NAD^+. Mol Cell. 2011;44:851–63.
15. Lee Y-H, Kim S-J, Fang X, Song N-Y, Kim D-H, Suh J, et al. JNK-mediated Ser27 phosphorylation and stabilization of SIRT1 promote growth and progression of colon cancer through deacetylation-dependent activation of Snail. Mol Oncol. 2022;16:1555–71.
16. Ford J, Ahmed S, Allison S, Jiang M, Milner J. JNK2-dependent regulation of SIRT1 protein stability. Cell Cycle. 2008;7:3091–7.
17. Nasrin N, Kaushik VK, Fortier E, Wall D, Pearson KJ, de Cabo R, et al. JNK1 phosphorylates SIRT1 and promotes its enzymatic activity. PLoS One. 2009;4:e8414.
18. Xu Y, Wan W. Acetylation in the regulation of autophagy. Autophagy. 2023;19:379–87.
19. Brown EE, Scandura MJ, Mehrotra S, Wang Y, Du J, Pierce EA. Reduced nuclear NAD^+ drives DNA damage and subsequent immune activation in the retina. Hum Mol Genet. 2022;31:1370–88.
20. Murnyák B, Kouhsari MC, Hershkovitch R, Kálmán B, Marko-Varga G, Klekner Á, et al. PARP1 expression and its correlation with survival is tumour molecular subtype dependent in glioblastoma. Oncotarget. 2017;8:46348–62.
21. Lu S, Wang XZ, He C, Wang L, Liang SP, Wang CC, et al. ATF3 contributes to brucine-triggered glioma cell ferroptosis via promotion of hydrogen peroxide and iron. Acta Pharmacol Sin. 2021;42:1690–702.
22. Zhou Z, Lu B, Wang C, Wang Z, Luo T, Piao M, et al. RIP1 and RIP3 contribute to shikonin-induced DNA double-strand breaks in glioma cells via increase of intracellular reactive oxygen species. Cancer Lett. 2017;390:77–90.
23. He C, Lu S, Wang XZ, Wang CC, Wang L, Liang SP, et al. FOXO3a protects glioma cells against temozolomide-induced DNA double strand breaks via promotion of BNIP3-mediated mitophagy. Acta Pharmacol Sin. 2021;42:1324–37.
24. Liu S, Luo W, Wang Y. Emerging role of PARP-1 and PARthanatos in ischemic stroke. J Neurochem. 2022;160:74–87.

25. Vermot A, Petit-Hartlein I, Smith SME, Fieschi F. NADPH oxidases (NOX): an overview from discovery, molecular mechanisms to physiology and pathology. Antioxidants. 2021;10:890.
26. Cheng F, Yuan W, Cao M, Chen R, Wu X, Yan J. Cyclophilin a protects cardiomyocytes against hypoxia/reoxygenation-induced apoptosis via the AKT/Nox2 pathway. Oxid Med Cell Longev. 2019;2019:2717986.
27. Wang Y, Ge X, Yu S, Cheng Q. Achyranthes bidentata polypeptide alleviates neurotoxicity of lipopolysaccharide-activated microglia via PI3K/Akt dependent NOX2/ROS pathway. Ann Transl Med. 2021;9:1522.
28. Hassa PO, Haenni SS, Buerki C, Meier NI, Lane WS, Owen H, et al. Acetylation of poly(ADP-ribose) polymerase-1 by p300/CREB-binding protein regulates coactivation of NF-kappaB-dependent transcription. J Biol Chem. 2005;280:40450–64.
29. Zhang L, Li D-Q. MORC2 regulates DNA damage response through a PARP1-dependent pathway. Nucleic Acids Res. 2019;47:8502–20.
30. Zhang ZX, Zhang WN, Sun YY, Li YH, Xu ZM, Fu WN. CREB promotes laryngeal cancer cell migration via MYCT1/NAT10 axis. Onco-Targets Ther. 2018;11:1323–31.
31. Huang M, Li X, Jia S, Liu S, Fu L, Jiang X, et al. Bisphenol AF induces apoptosis via estrogen receptor beta (ERbeta) and ROS-ASK1-JNK MAPK pathway in human granulosa cell line KGN. Environ Pollut. 2021;270:116051.
32. Ying W. NAD^+ and NADH in cellular functions and cell death. Front Biosci. 2006;11:3129–48.
33. Alaee M, Khaghani S, Behroozfar K, Hesari Z, Ghorbanhosseini SS, Nourbakhsh M. Inhibition of nicotinamide phosphoribosyltransferase induces apoptosis in estrogen receptor-positive MCF-7 breast cancer cells. J Breast Cancer. 2017;20:20–6.
34. Yang P, Zhang L, Shi QJ, Lu YB, Wu M, Wei EQ, et al. Nicotinamide phosphoribosyltransferase inhibitor APO866 induces C6 glioblastoma cell death via autophagy. Pharmazie. 2015;70:650–5.
35. Pajuelo D, Gonzalez-Juarbe N, Tak U, Sun J, Orihuela CJ, Niederweis M. NAD^+ depletion triggers macrophage necroptosis, a cell death pathway exploited by *Mycobacterium tuberculosis*. Cell Rep. 2018;24:429–40.
36. Martínez-Morcillo FJ, Cantón-Sandoval J, Martínez-Navarro FJ, Cabas I, Martínez-Vicente I, Armistead J, et al. NAMPT-derived NAD^+ fuels PARP1 to promote skin inflammation through parthanatos cell death. PLoS Biol. 2021;19:e3001455.
37. Zheng T, Zheng CY, Zheng XC, Zhao RG, Chen YQ. Effect of parthanatos on ropivacaine-induced damage in SH-SY5Y cells. Clin Exp Pharmacol Physiol. 2017;44:586–94.
38. Lu P, Kamboj A, Gibson SB, Anderson CM. Poly(ADP-ribose) polymerase-1 causes mitochondrial damage and neuron death mediated by Bnip3. J Neurosci. 2014;34:15975–87.
39. Ying W, Garnier P, Swanson RA. NAD^+ repletion prevents PARP-1-induced glycolytic blockade and cell death in cultured mouse astrocytes. Biochem Biophys Res Commun. 2003;308:809–13.
40. Carnevale I, Pellegrini L, D'Aquila P, Saladini S, Lococo E, Polletta L, et al. SIRT1-SIRT3 axis regulates cellular response to oxidative stress and etoposide. J Cell Physiol. 2017;232:1835–44.
41. Chai R, Fu H, Zheng Z, Liu T, Ji S, Li G. Resveratrol inhibits proliferation and migration through SIRT1 mediated post-translational modification of PI3K/AKT signaling in hepatocellular carcinoma cells. Mol Med Rep. 2017;16:8037–44.
42. Shi Z, Yao J, Ma X, Xu D, Ming G. CUL5-mediated visfatin (NAMPT) degradation blocks endothelial proliferation and angiogenesis via the MAPK/PI3K-AKT signaling. J Cardiovasc Pharmacol. 2021;78:891–9.
43. Vallejo FA, Sanchez A, Cuglievan B, Walters WM, De Angulo G, Vanni S, et al. NAMPT inhibition induces neuroblastoma cell death and blocks tumor growth. Front Oncol. 2022;12:883318.
44. Zhao C, Li W, Duan H, Li Z, Jia Y, Zhang S, et al. NAD^+ precursors protect corneal endothelial cells from UVB-induced apoptosis. Am J Physiol Cell Physiol. 2020;318:C796–C805.
45. Cao Y, Yao M, Wu Y, Ma N, Liu H, Zhang B. N-Acetyltransferase 10 promotes micronuclei formation to activate the senescence-associated secretory phenotype machinery in colorectal cancer cells. Transl Oncol. 2020;13:100783.
46. Dalhat MH, Altayb HN, Khan MI, Choudhry H. Structural insights of human N-acetyltransferase 10 and identification of its potential novel inhibitors. Sci Rep. 2021;11:6051.
47. Wang K, Zhou LY, Liu F, Lin L, Ju J, Tian PC, et al. PIWI-Interacting RNA HAAPIR regulates cardiomyocyte death after myocardial infarction by promoting NAT10-Mediated ac(4) C ACETYLATION Of Tfec mRNA. Adv Sci. 2022;9:e2106058.
48. Liu H, Ling Y, Gong Y, Sun Y, Hou L, Zhang B. DNA damage induces N-acetyltransferase NAT10 gene expression through transcriptional activation. Mol Cell Biochem. 2007;300:249–58.
49. Jeong H, Cohen DE, Cui L, Supinski A, Savas JN, Mazzulli JR, et al. Sirt1 mediates neuroprotection from mutant huntingtin by activation of the TORC1 and CREB transcriptional pathway. Nat Med. 2011;18:159–65.
50. Ma S, Yeom J, Lim YH. Exogenous NAD^+ stimulates MUC2 expression in LS 174T goblet cells via the PLC-delta/PTGES/PKC-delta/ERK/CREB signaling pathway. Biomolecules. 2020;10:580.
51. Kim YM, Park EJ, Kim HJ, Chang KC. Sirt1 S-nitrosylation induces acetylation of HMGB1 in LPS-activated RAW264.7 cells and endotoxemic mice. Biochem Biophys Res Commun. 2018;501:73–9.
52. Shinozaki S, Chang K, Sakai M, Shimizu N, Yamada M, Tanaka T, et al. Inflammatory stimuli induce inhibitory S-nitrosylation of the deacetylase SIRT1 to increase acetylation and activation of p53 and p65. Sci Signal. 2014;7:ra106.
53. Sun HJ, Xiong SP, Cao X, Cao L, Zhu MY, Wu ZY, et al. Polysulfide-mediated sulfhydration of SIRT1 prevents diabetic nephropathy by suppressing phosphorylation and acetylation of p65 NF-kappaB and STAT3. Redox Biol. 2021;38:101813.
54. Yu L, Dong L, Li H, Liu Z, Luo Z, Duan G, et al. Ubiquitination-mediated degradation of SIRT1 by SMURF2 suppresses CRC cell proliferation and tumorigenesis. Oncogene. 2020;39:4450–64.
55. Sasaki T, Maier B, Koclega KD, Chruszcz M, Gluba W, Stukenberg PT, et al. Phosphorylation regulates SIRT1 function. PLoS One. 2008;3:e4020.
56. Lau AW, Liu P, Inuzuka H, Gao D. SIRT1 phosphorylation by AMP-activated protein kinase regulates p53 acetylation. Am J Cancer Res. 2014;4:245–55.
57. Kang H, Jung J-W, Kim MK, Chung JH. CK2 is the regulator of SIRT1 substrate-binding affinity, deacetylase activity and cellular response to DNA damage. PLoS One. 2009;4:e6611.
58. Chang CY, Pan PH, Wu CC, Liao SL, Chen WY, Kuan YH, et al. Endoplasmic reticulum stress contributes to gefitinib-induced apoptosis in glioma. Int J Mol Sci. 2021;22:3934.
59. Zheng L, Wang C, Luo T, Lu B, Ma H, Zhou Z, et al. JNK activation contributes to oxidative stress-induced parthanatos in glioma cells via increase of intracellular ROS production. Mol Neurobiol. 2017;54:3492–505.
60. Wang C, He C, Lu S, Wang X, Wang L, Liang S, et al. Autophagy activated by silibinin contributes to glioma cell death via induction of oxidative stress-mediated BNIP3-dependent nuclear translocation of AIF. Cell Death Dis. 2020;11:630.